interdigital transducers," *IEEE Trans. Sonics Ultrason.*, vol. SU-24, pp. 147–166, May 1977.
[47] W. S. Mortley, "F.M.Q.," *Wireless World*, vol. 57, pp. 399–403, Oct. 1951.
[48] ——, "Frequency-modulated quartz oscillators for broadcasting equipment," *Proc. Inst. Elect. Eng.*, vol. 104B, pp. 239–249, Dec. 1956.
[49] ——, "Priority in energy trapping," *Phys. Today*, vol. 19, pp. 11–12, Dec. 1966.
[50] W. H. Horton and R. C. Smythe, "The work of Mortley and the energy-trapping theory for thickness-shear piezoelectric vibrators," *Proc. IEEE*, vol. 55, p. 222, Feb. 1967.
[51] W. Shockley, D. R. Curran, and D. J. Koneval, "Energy trapping and related studies of multiple electrode filter crystals," in *Proc. 17th Annual Frequency Control Symp.*, pp. 88–126, May 1963.
[52] ——, "Trapped-energy modes in quartz filter crystals," *J. Acoust. Soc. Amer.*, vol. 41, pp. 981–993, Apr. 1967.
[53] R. D. Mindlin, "Bechmann's number for harmonic overtones of thickness/twist vibrations of rotated-*Y*-cut quartz plates," *J. Acoust. Soc. Amer.*, vol. 41, pp. 969–973, Apr. 1967.
[54] A. A. Oliner, "Microwave network methods for guided elastic waves," *IEEE Trans. Microwave Theory Tech.*, vol. MTT-17, pp. 812–826, Nov. 1969.
[55] E. A. Ash, R. M. De La Rue, and R. F. Humphryes, "Microsound surface waveguides," *IEEE Trans. Microwave Theory Tech.*, vol. MTT-17, pp. 882–892, Nov. 1969.
[56] H. F. Tiersten, "Elastic surface waves guided by thin films," *J. Appl. Phys.*, vol. 40, pp. 770–789, Feb. 1969.
[57] H. F. Tiersten and R. C. Davis, "Elastic surface waves guided by curved thin films," *J. Appl. Phys.*, vol. 44, pp. 2097–2112, May 1973.
[58] B. K. Sinha and H. F. Tiersten, "Elastic and piezoelectric surface waves guided by thin films," *J. Appl. Phys.*, pp. 4831–4854, vol. 44, Nov. 1973.
[59] M. F. Lewis, private communication, Feb. 1979.
[60] E. C. Jordan, *Electromagnetic Waves and Radiating Systems*. Englewood Cliffs, NJ: Prentice-Hall, 1950, pp. 391–450.
[61] E. I. Jury, *Theory and Application of the z-Transform Method*. New York: Wiley, 1964.
[62] P. M. DeRusso, R. J. Roy, and C. M. Close, *State Variables for Engineers*. New York: Wiley, 1965, pp. 158–186.
[63] H. Gautier and G. S. Kino, "A detailed theory of the acoustic wave semiconductor convolver," *IEEE Trans. Sonics Ultrason.*, vol. SU-24, pp. 23–33, Jan. 1977.
[64] B. T. Khuri-Yakob and G. S. Kino, "A detailed theory of the monolithic zinc oxide on silicon convolver," *IEEE Trans. Sonics Ultrason.*, vol. SU-24, pp. 34–43, Jan. 1977.
[65] E. P. EerNisse, T. Lukaszek, and A. Ballato, "Variational calculation of force-frequency constants of doubly rotated quartz resonators," *IEEE Trans. Sonics Ultrason.*, vol SU-25, pp. 132–138, May 1978.
[66] A. Ballato, "Static and dynamic behavior of quartz resonators," *IEEE Trans. Sonics Ultrason.*, vol. SU-26, July 1979, pp. 299–306.
[67] J. R. Vig, J. W. LeBus and R. L. Filler, "Chemically polished quartz," in *Proc. 31st Annual Frequency Control Symp.*, pp. 131–143, June 1977.
[68] B. A. Auld, J. J. Gagnepain, and M. Tan, "Horizontal shear surface waves on corrugated surfaces," *Electron. Lett.*, vol. 12, pp. 650–652, Nov. 1976.
[69] Y. V. Gulyaev and V. P. Plessky, *Pis'ma v Zh. Tekh. Fiz.* (USSR), vol. 3, pp. 20 ff. 1977. (Transl., *Sov. Tech. Phys. Lett.* (USA), vol. 3, pp. 87 ff, 1977.)

Practical Aspects of Surface-Acoustic-Wave Oscillators

S. K. SALMON

Abstract—**A surface-acoustic-wave (SAW) delay line integrated with a thin film amplifier can form the basis of a small high-stability microwave oscillator. Practical aspects of delay lines and the noise properties, stabilization, frequency setting, and modulation of oscillators are presented.**

I. Introduction

THE surface-acoustic-wave (SAW) oscillator has a stability comparable to that of a bulk crystal-locked oscillator but since it can operate at a very much higher frequency, problems associated with harmonics, when deriving higher frequencies by frequency multiplication, are therefore reduced. It can also be frequency modulated. Compared to a phase-locked oscillator it has a wide-band low-noise spectrum. The SAW delay line can readily be integrated with a thin film amplifier to form a small high-stability oscillator, presently at frequencies of up to approximately 1.5 GHz. Therefore, the potential of SAW oscillators is attractive and they are now being considered for communications and navigation systems for both transmitter sources and receiver local oscillators.

In this paper it is intended to outline the basic principles and performance of SAW oscillators and the factors affecting the frequency stability, both over an operating temperature range and in the long term, the oscillator sideband noise, the accuracy of frequency setting, and the deviation and maximum rate of frequency modulation.

Manuscript received April 27, 1979; revised October 11, 1979.
The author is with Philips Research Laboratories, Redhill, Surrey, England.

0018-9480/79/1200-1012$00.75 ©1979 IEEE

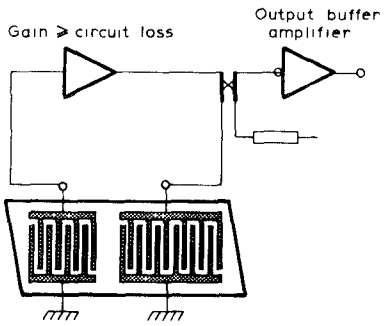

Fig. 1. SAW oscillator.

A SAW oscillator [1] is basically an amplifier with a multiwavelength SAW delay line path from output to input (Fig. 1). The low velocity of the SAW makes it ideal as a delay line suitable for integration with other thin film components. The upper frequency is limited by photolithography techniques; e.g., with $\lambda = 3.2$ μm at approximately 1 GHz, line widths of 0.8 μm need to be defined in the transducer metal pattern.

II. Conditions for Oscillation

The gain of the amplifier must be greater than circuit losses. In practice, at UHF, loss of the delay line with both transducers power matched, is typically 17 dB. Some power is extracted by the load, so a typical amplifier gain might be 24 dB, allowing excess gain.

The frequency of oscillation must satisfy the condition

$$2n\pi = 2\pi f \frac{l}{v} + \phi_e \tag{1}$$

where

- n an integer,
- l the SAW line length,
- v the velocity,
- ϕ_e the remaining loop phase shift.

Assuming the delay line is stable, the frequency deviation is

$$\Delta f = -\Delta\phi \frac{v}{2\pi l}. \tag{2}$$

The oscillator stability increases with greater length l, giving a large value of n. As n is increased the frequency separation between possible modes of oscillation decreases, i.e., $f_{n+1} - f_n = f_n/n$. For most applications it is necessary to limit the oscillator to a single mode, and the delay line is therefore designed to have a narrow-band filter characteristic.

III. Oscillator Noise

The plateau noise of the oscillator, away from the frequency where the filter characteristic of the SAW delay line has any influence, is the amplifier output noise. This is approximately

$$N_p = 10\log_{10}\left[\frac{G_k^2 T_0 F}{P_0}\right] \text{dBc/Hz}. \tag{3}$$

where

- G^2 the power gain of the amplifier,
- F the operational noise figure,
- P_0 the saturated output power of the amplifier,
- dBc dB relative to P_0 (the carrier power).

In practice the source impedance may be a large mismatch and would be purely reactive but for circuit and transducer losses. It is shown (Appendix I) that the noise power output could be reduced under reactive source conditions if the source reactance were the optimum value for minimum amplifier noise figure. In practice the losses must be included when considering the amplifier source impedance, and care must be taken in the circuit design to avoid the amplifier operating under source impedance conditions which would result in high output noise. In communications systems with superheterodyne receivers the plateau noise should be minimized at IF offsets from the carrier frequency in order to minimize system noise.

Further, the gain of the amplifier, at the oscillation frequency, is compressed to equal the loss in the oscillator feedback circuit and the small signal gain, at plateau frequencies, is compressed by an amount which depends on the saturation characteristic. For example, we have shown by detailed measurements on a Mullard OM 335 amplifier module that with a large signal gain compression of 4 dB a small signal is compressed by 9 dB, and at larger signals this excess small signal compression remains approximately 5 dB. Such an amplifier is suitable for giving low plateau noise in SAW oscillators. However, experimental laboratory amplifiers without a sharp limiting characteristic have been measured and show small signal gain compression significantly less than the large signal saturation compression. This indicates that care must be taken in the choice of amplifier. Hence the qualification that (3) gives the approximate value.

The phase noise sideband spectral density at offset Δf, relative to carrier power at frequency f_0, is shown in Appendix II to be given by

$$\mathcal{L}(f) = 10\log_{10}\left[\frac{G^2 k T_0 F f_0^2}{4\pi^2 n^2 P_0 \Delta f^2}\right] \text{dBc/Hz}. \tag{4}$$

From (4) it is apparent that the lowest noise performance will be obtained if the delay line loss is minimized and a low-noise high-power amplifier is used with a long delay line. However, the tuning range, which can be achieved by external phase shift, given in (2), is inversely proportional to length.

A low level of close to carrier noise is generally desirable for both transmitter and local oscillator in wide dynamic range communications systems. It is also important in multichannel systems because part of the noise sideband of a large signal may come into the received bandwidth of a smaller adjacent channel and hence reduce dynamic range.

The noise performance of an oscillator is shown in Fig. 2. The results (o) closest to carrier were obtained with an

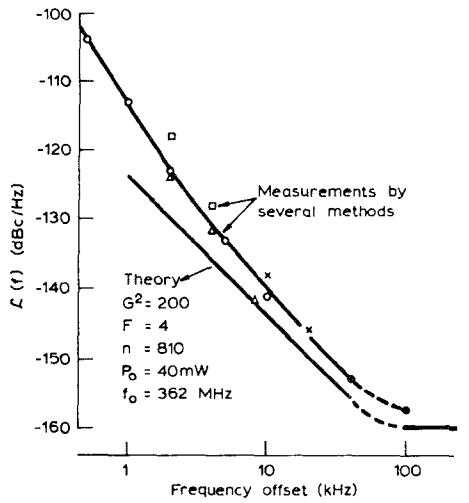

Fig. 2. Phase noise sideband spectral density of a SAW oscillator.

Adret Electronique spectrum analyzer type 6306 (with 63032 analysis head). The input to the Adret was the 4-MHz IF output of a mixer fed by two similar SAW oscillators. The remaining results were obtained by taking the outputs of two locked oscillators and introducing a 90°-phase difference before applying to a doubly balanced mixer and then displaying the output on a spectrum analyzer [2]. The results were obtained with different analyzer bandwidths. The phase difference could be varied and 90° gave the maximum noise output. 0°, which corresponds to amplitude noise detection, gave 10- to 15-dB lower noise output, confirming that the noise output was predominately phase noise. The level of locking signal was varied to confirm that it was below the level which would affect the noise measurements.

At frequency offsets greater than 5 kHz the results are within 3 dB of theory. At lower frequencies the slope increases from $1/f^2$ to $1/f^3$. This $1/f$ addition is typical of most oscillators [3] and Parker [4] attributes this to the SAW transducers.

IV. Filter Design and Construction

The SAW is launched in the piezoelectric material by transducers of a thin metal film interdigital structure where common polarity fingers are a wavelength apart (Fig. 1). The filter characteristic is obtained by designing [5] on the principles of an interferometry array. A long transducer is required to give a narrow bandpass characteristic. A transducer mechanically loads the surface and causes attenuation and slowing of the wave. Further, loading of the surface causes reflections within the transducer which distorts the passband [6]. This is minimized by thinning the structure which has the added advantage of giving less slowing and attenuation of the wave.

A structure of this type (Fig. 3(a), transducer L) consists of a number of equally spaced groups of finger pairs. It resembles a ladder structure and the groups are usually referred to as rungs. On quartz a rung will typically consist of ten finger pairs. This transducer gives a comb of frequencies (Fig. 3(b)). The next possible oscillatory

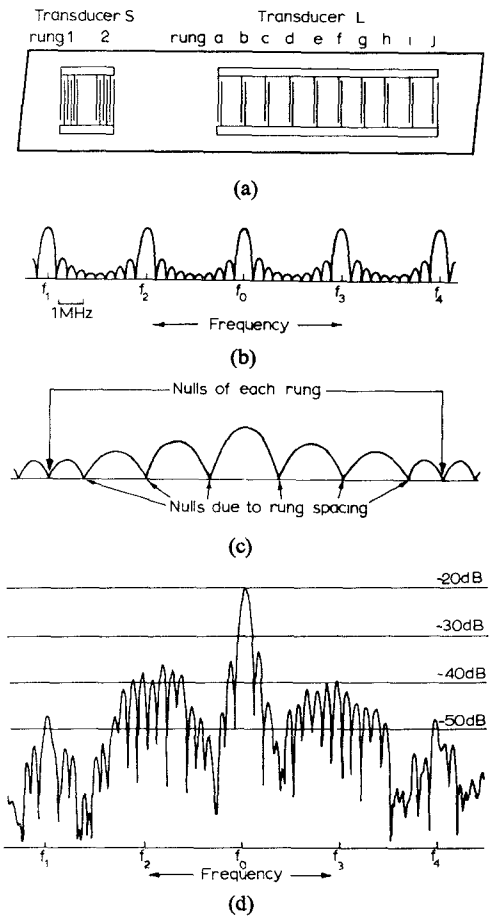

Fig. 3. Delay line and associated frequency responses. (a) Delay line with ladder transducers. (b) Frequency response of transducer L. (c) Frequency response of transducer S. (d) Measured frequency response of delay line.

modes ($n \pm 1$) coincide with the first nulls. The other transducer S is designed to select a frequency of the comb and give nulls at the remainder (Fig. 3(c)). Fig. 3(d) shows the measured frequency/amplitude response of a delay line of this design centered at approximately 400 MHz. All possible undesired oscillatory modes are well suppressed by this filter. The SAW velocities for parts of the structure were initially estimated from Slobodnik's data [7] and then corrected in a second mask design. We have demonstrated multifrequency operation by selecting other frequencies of the comb by placing additional transducers at both ends of the ladder transducer and then electronically switching.

For a lossless structure the delay line length is between transducer centers. In practice a spread of the delay is found in production due to the phase center of the transducer not being at the physical center because of imperfections and attenuation under the length of the transducer. This shortening of the delay line has been measured at 400 MHz and 1 GHz to be approximately 7 percent. The photograph (Fig. 4) shows the transient response in the time domain of a 400-MHz delay line of the design illustrated in Fig. 3(a). The first response is due to the closest pair of rungs in the two rung transducer (S rung 2) and the ladder transducer (L rung a). It is indicated thus on the photograph that this response is from

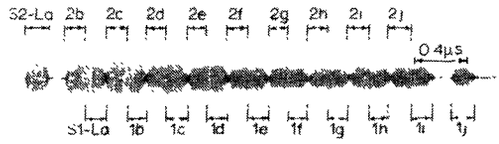

Fig. 4. Transient response of a 400-MHz delay line with the two transducers having 10 and 2 rungs.

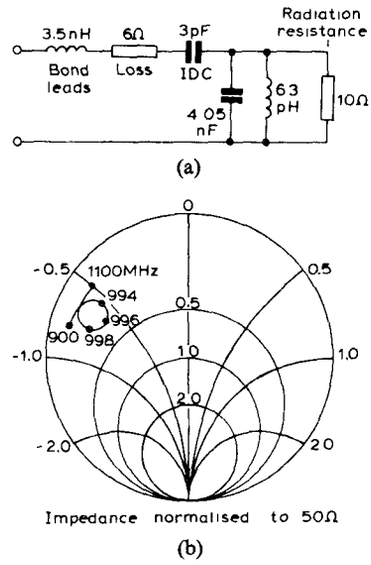

Fig. 5. (a) Equivalent circuit of IDT. (b) Impedance locus 900 to 1100 MHz.

the pair $S2$-La. The key to the remainder of the response is similarly indicated but shortened from ($S2$-Lb) to $2b$.

Long-term frequency stability (aging) is currently between 2 and 10 ppm/year. The larger value is for current production devices which are mounted in a dry nitrogen atmosphere in an outgassed To8 encapsulation. Volatile materials, which contaminate the surface, are avoided. Aging rates as low as 2 ppm are being measured in the laboratory on devices loosely mounted without mechanical stresses in an evacuated glass envelope.

The simple equivalent circuit of an interdigital transducer (IDT) at 1 GHz is shown in Fig. 5(a). The bond-lead inductance was estimated and the interdigital capacitance calculated [8], [9]. The values of these were confirmed by broad-band measurements; similarly the series loss was taken as the real part of the impedance locus at 900 and 1100 MHz (Fig. 5(b)). Over the passband of the filter the impedance locus shows a shunt resonant loop extending over approximately 10 MHz. The values of the shunt resonant elements were chosen to fit the measured impedance.

At present the most stable oscillators are made on quartz by evaporation of approximately 1000 Å of aluminium followed by photolithographic pattern definition. Reproducibility depends on carefully controlling the metal thickness and mark/space ratio. Using a thinned transducer structure also aids reproducibility. A few faults have insignificant effects.

For an ST cut of quartz, with propagation in the X direction a typical stability is 40 ppm for an operating temperature range of -10 to 60°C. To improve stability

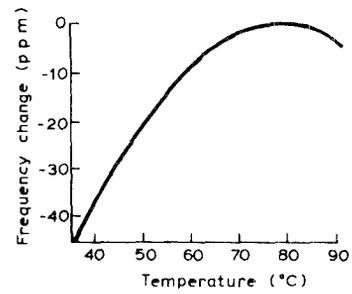

Fig. 6. Frequency change v temperature. AT cut quartz (35° 06′).

an AT cut slice can be temperature controlled and Fig. 6 shows a measured characteristic of frequency against surface temperature for a cut of 35° 06′. The temperature needs only to be controlled to ±5°C at the peak of the parabolic characteristic to achieve a stability of 1 ppm for the quartz. Amplifier phase shift will then tend to dominate; e.g., for a Mullard OM 337 amplifier the phase shift is $-7°$ for 0 to 60°C, resulting in 20-ppm frequency change with a 1000-λ delay line. Overall stability of approximately 5 ppm can be achieved with the quartz temperature controlled and with the amplifier phase compensated. This is comparable with uncontrolled bulk crystal oscillators at HF. Browning and Lewis [10] have demonstrated compensation of a delay line by a composite delay line structure giving ±15 ppm from -40 to $+100$°C.

V. Frequency Setting and Tuning

Provided the filter response encompasses the required frequency, accurate frequency setting can be achieved by a combination of the following:

a) π phase change by reversing connections to one transducer,
b) external transmission lines of up to $\lambda/4$,
c) triming capacitors in external circuit.

Frequency setting accuracy has been achieved in the laboratory to ±3 ppm.

VI. Frequency Modulation

The trimming capacitor can be a varactor, and a phase shift of 40° can be obtained from a single varactor with resonating inductor to restrict the mismatch to $<2:1$. This gives a total deviation of $f_0/10n$. This range can be doubled by a network with two or more varactors.

The rate at which the frequency can be changed by a voltage step is dependent on the delay (τ) and a new frequency can be established for the same mode in $<3\tau$. For square wave modulation, therefore, 1 cycle takes 6τ. Approximately 10τ is required for sinusoidal modulation according to Lewis [1].

Appendix I

The noise output [11] from an amplifier with noise figure F is given by

$$N_p = N_S + N_{\text{int}} = FN_S \qquad \text{(A1)}$$

where N_S is the portion of the total noise power at the output due to the source impedance at T_0, standard tem-

perature, and N_{int} is the portion due to the noise generated internally. If the amplifier is matched to the source, the noise power per unit bandwidth due to the source resistance is the available power kT_0. Where k is Boltzmann's constant. The noise power out is thus

$$N_p = FkT_0 g_T \text{ per unit bandwidth} \tag{A2}$$

where g_T is the gain of the amplifier into a load R_L when the input is matched.

For a current source i_s of admittance $G_S + jB_S$ feeding an amplifier with input admittance $G_{in} + jB_{in}$, the power dissipated in G_{in} is given by

$$P_{in} = \frac{i_{in} \times i_{in}^*}{G_{in}} \tag{A3}$$

where i_{in} is the input current to the amplifier and i_{in}^* the conjugate.

$$\therefore \quad P_{in} = \frac{G_{in} i_S^2}{\left[(G_S + G_{in})^2 + (B_S + B_{in})^2\right]}. \tag{A4}$$

For the power matched condition, $G_S = G_{in}$ and $B_S = -B_{in}$, the maximum power transfer to the amplifier is

$$P_{max} = \frac{i_S^2}{4G_S}. \tag{A5}$$

Defining the power transfer ratio as

$$P_T = \frac{P_{in}}{P_{max}}$$

$$\therefore \quad P_T = \frac{4G_S G_{in}}{\left[(G_S + G_{in})^2 + (B_S + B_{in})^2\right]}. \tag{A6}$$

$\therefore$ Amplifier gain is

$$g = g_T P_T$$

$$g = g_T \frac{4G_S G_{in}}{\left[(G_S + G_{in})^2 + (B_S + B_{in})^2\right]}. \tag{A7}$$

At a specified frequency the noise figure of an amplifier is given by [12]

$$F = F_{min} + \frac{R_n}{G_S}\left[(G_S - G_0)^2 + (B_S - B_0)^2\right] \tag{A8}$$

where F_{min} is the minimum noise figure, R_n is a parameter known as "the equivalent noise resistance," and $Y_0 = G_0 + jB_0$ is the source admittance for F_{min}. These amplifier parameters can be measured [13].

The noise power output (A1) per unit bandwidth for an amplifier not matched to its source is

$$N_P = FkT_0 g \tag{A9}$$

from (A7) and (A8).

$$N_P = kT_0 g_T \cdot \left[\frac{4G_S G_{in} F_{min} + 4R_n G_{in}\left[(G_S - G_0)^2 + (B_S - B_0)^2\right]}{(G_S + G_{in})^2 + (B_S + B_{in})^2}\right]. \tag{A10}$$

As an example the parameters of an Avantek AT4641 transistor were measured and substituted in the above (A9) and (A10) for an amplifier with a 55-dB gain.

For a 50-Ω source resistance the power output in a 300-kHz bandwidth was calculated to be −62 dBm and measured to be −61 dBm. For a short circuit source ($G_S = \infty, B_S = 0$) the power was calculated to be −65.1 dBm and measured to be −64 dBm. For an open circuit source ($G_S = 0, B_S = 0$) the power was calculated to be −66 dBm and measured to be −62 dBm.

With a variable length 50-Ω line terminated in a short circuit the maximum power output was −60 dBm and the minimum −67 dBm.

These figures indicate that there is reasonable agreement between theory and practice (it is difficult to provide an open-circuit source, which may explain the one departure), and oscillator plateau noise could vary by up to 7 dB for this transistor type.

Appendix II

Feedback Oscillator Noise Spectrum

The noise theory presented by Lewis [1] is here expanded and provides an expression for $\mathcal{L}(f)$, the phase noise sideband spectral density normalized to carrier power, in dBc/Hz. This is derived as a function of frequency offset from carrier for an oscillator stabilized by a SAW delay line. $\mathcal{L}(f)$ is then related [14], [15] to the standard expression [16], [3] $S_\phi(\omega)$, the spectral density of $\phi(t)$ the instantaneous phase angle, in rad^2/Hz.

The following assumptions are made.

a) The amplifier is broad band and limits in oscillation by reducing its gain uniformly at all frequencies.
b) The oscillator frequency f_0 is the center frequency of the transducers and $2\pi f_0 \tau = \omega_0 \tau = 2n\pi$, where τ is feedback delay time.
c) The RF spectral bandwidth is small compared to the filter bandwidth of the transducers and the loss is constant over the spectral bandwidth.
d) The amplifier acts as an isolator ensuring waves travel around the loop in one direction only.
e) Other possible modes of the oscillator loop coincide with nulls of the transducer characteristics.

Imagine the oscillator (Fig. 1) is below threshold and an input signal $V\exp(j\omega t)$ is injected at the input to the amplifier. The output will be given by

$$V_0(\omega) = GV\left[\exp(j\omega t) + A\exp(j\omega(t-\tau)) + A^2\exp(j\omega(t-2\tau)) \cdots + A^n \exp(j\omega(t-n\tau)) \cdots\right] \tag{A11}$$

$$A = GL$$

where

A the amplitude transmission factor of the loop
G amplifier voltage gain
L delay line voltage loss

from (A11)

$$V_0(\omega) = GV\exp(j\omega t)(1 + A\exp(-j\omega\tau) + A^2\exp(-j\omega 2\tau) \cdots + A^n\exp(-j\omega n\tau)\cdots) \quad \text{(A12)}$$

$$= \frac{GV\exp(j\omega t)}{(1 - A\exp(-j\omega\tau))}. \quad \text{(A13)}$$

The output power of the amplifier into a matched load is

$$P(\omega) = \frac{V_0(\omega) \times V_0(\omega)^*}{R_0}$$

where

$V_0(\omega)^*$ the conjugate of $V_0(\omega)$

R_0 the output resistance of the amplifier.

$$P(\omega) = \frac{G^2V^2(\exp(j\omega t) \times \exp(-j\omega t))}{R_0(1 - A\exp(-j\omega\tau))(1 - A\exp(j\omega\tau))}$$

$$= \frac{G^2V^2}{R_0}\left[\frac{1}{1 + A^2 - 2A\cos\omega\tau}\right]$$

$\cos\omega\tau = \cos(\omega\tau - 2n\pi)$

from assumption b) $\omega_0\tau = 2n\pi$

$\therefore \cos\omega\tau = \cos(\omega - \omega_0)\tau$

$$\therefore P(\omega) = \frac{G^2V^2}{R_0}\left[\frac{1}{1 + A^2 - 2A\cos(\omega - \omega_0)\tau}\right]. \quad \text{(A14)}$$

If P_0 is the saturated output power of the amplifier and the spectrum is within the range $\omega = \omega_0 \pm \pi/\tau$

$$P_0 = \frac{\tau}{2\pi}\int_{\omega_0 - \pi/\tau}^{\omega_0 + \pi/\tau} P(\omega)\, d\omega$$

$$P_0 = \frac{\tau G^2V^2}{2\pi R_0}\int_{\omega_0 - \pi/\tau}^{\omega_0 + \pi/\tau} \frac{d\omega}{1 + A^2 - 2A\cos(\omega - \omega_0)\tau}. \quad \text{(A15)}$$

This integral is of a standard form

$$\int \frac{dx}{a + b\cos x} = \left[\frac{2}{\sqrt{a^2 - b^2}}\tan^{-1}\frac{(a - b)\tan x/2}{\sqrt{a^2 - b^2}}\right]$$

substituting $a = 1 + A^2$, $b = -2A$, $x = (\omega - \omega_0)\tau$, and $d\omega = dx/\tau$.

$$\therefore P_0 = \frac{\tau G^2V^2 2\pi}{2\pi R_0\tau\sqrt{(1 + A^2)^2 - (-2A)^2}} \quad \text{(A16)}$$

$$= \frac{G^2V^2}{R_0(1 - A^2)}$$

$$\therefore 1 - A^2 = \frac{G^2V^2}{R_0P_0}. \quad \text{(A17)}$$

If A approaches unity then

$1 - A^2 \approx 2(1 - A)$ is a good approximation. (A18)

Substituting the values for A^2 and A, derived from (A17) and (A18), (A14) gives

$$P(\omega) = \frac{G^2V^2}{R_0}\left[\frac{1}{\left(2 - \frac{G^2V^2}{R_0P_0}\right)(1 - \cos\Delta\omega\tau)}\right] \quad \text{(A19)}$$

where

$$\Delta\omega = \omega - \omega_0.$$

The equivalent mean-squared input voltage to the amplifier with input power matched is

$$\overline{V^2} = \frac{4kT_0BRF}{4}. \quad \text{(A20)}$$

This assumes the amplifier is noiseless and the internal noise from the amplifier (with noise figure F) is present at the input.

If $R = R_0$ (A19) becomes

$$P(\omega) = G^2kT_0BF\left[\frac{1}{\left(2 - \frac{G^2kT_0F}{P_0\tau}\right)(1 - \cos\Delta\omega\tau)}\right]. \quad \text{(A21)}$$

Now

$$\cos\theta = 1 - \frac{\theta^2}{2!} + \frac{\theta^4}{4!}\cdots$$

for small values of θ,

$$1 - \cos\theta \approx \frac{\theta^2}{2}$$

$$\therefore P(\omega) = \frac{G^2kT_0BF}{\left(2 - \frac{G^2kT_0F}{P_0\tau}\right)\frac{\Delta\omega^2\tau^2}{2}}$$

since

$$\frac{G^2kT_0F}{P_0\tau} \ll 2 \text{ and } \tau = \frac{2\pi n}{\omega_0}$$

$$P(\omega) = \frac{G^2kT_0BF\omega_0^2}{4\pi^2n^2\Delta\omega^2}$$

or

$$P(f) = \frac{G^2kT_0Ff_0^2}{4\pi^2n^2\Delta f^2}\text{ W/Hz}. \quad \text{(A22)}$$

The phase noise sideband spectral density at offset Δf from carrier frequency f_0 relative to carrier power P_0 is therefore given

$$\mathcal{L}(f) = 10\log_{10}\left[\frac{G^2kT_0Ff_0^2}{4\pi^2n^2P_0\Delta f^2}\right]\text{dBc/Hz}. \quad \text{(A23)}$$

This expression has been derived in terms (A20) of the noise power kT_0 from a resistor (i.e. $\tau\ \overline{V^2}/4R$) and differs from that of Lewis who has a factor $4kT_0$ in his expression (F_{ssb}).

$\mathcal{L}(f)$ is approximately related [14], [15] to the standard expression for the spectral density of $\phi(t)$ the instantaneous phase angle by

$$S_\phi(f) = 2\mathcal{L}(f)\,\text{rad}^2/\text{Hz}.$$

One method by which this noise $\mathcal{L}(f)$, can be measured is to sweep slowly a narrow-band filter through the spectrum. This was the case when measurements described in the text were made with the Adret spectrum analyzer which has a filter bandwidth of 10 Hz. The measurement approaches the theoretical value given by (A23) when the error introduced by summing in a larger bandwidth (10 Hz) becomes small at larger offset frequencies. An alternative method of measurement is to analyze the phase modulation sideband by taking the outputs of two locked oscillators and introducing a 90°-phase difference before applying to a doubly balanced mixer [2]. This mixer is then a phase detector and the "power" measured using the Hewlett Packard calibration [2] (6-dB setting) is the same as above. This method of measurement assumes one oscillator is noiseless relative to the one under test. In practice measuring SAW oscillators, which have very low phase noise, it is usual to use two identical oscillators and, therefore, since their noise is uncorrelated, 3 dB is subtracted from the measurement to give the sideband noise of a single oscillator.

Acknowledgment

The design of delay lines, the transient response measurements, and the basis of the derivation of the noise equations were performed by colleagues R. Stevens and R. N. Bates. R. I. H. Scott provided the necessary guidance relating Appendix II to noise standards. The accurately reproduced SAW delay lines have been made by P. Mayor of the Central Materials Laboratory, Mullard Mitcham, Surrey. Discussions with Dr. M. F. Lewis of RSRE Malvern have proved to be valuable.

References

[1] M. F. Lewis, "Surface acoustic wave devices and applications—6 oscillators," *Ultrasonics*, p. 115, May 1974.
[2] "Spectrum analysis—noise measurements," Hewlett-Packard Application Note 150-4, Jan. 1973.
[3] D. B. Leeson, "A simple model of feedback oscillator noise spectrum," *Proc. IEEE*, vol. 54, p. 329–330, Feb. 1966.
[4] T. E. Parker, "1/f phase noise in quartz SAW devices," *Electron. Lett.*, vol. 15, no. 10, p. 296–298, May 1979.
[5] W. R. Smith, H. M. Gerard, J. H. Collins, T. M. Reeder, and H. J. Shaw, "Design of surface wave delay lines with interdigital transducers," *IEEE Trans. Microwave Theory Tech.*, vol. MTT-17, p. 865–873, 1969.
[6] H. Skeie, "Mechanical and electrical reflections in interdigital transducers," *IEEE Ultrason. Symp. Proc.*, p. 408–412, 1972.
[7] A. J. Slobodnik, E. D. Conway, and R. T. Delmonico, "Surface wave velocities," *Microwave Acoustics Handbook*, vol. 1A, AFCRL-TR-73-0597, 1973.
[8] Y. C. Lim, and R. A. Moore, "Properties of alternately charged coplanar strips by conformal mappings," *IEEE Trans. Electron Dev.*, vol ED-15, Mar. 1968.
[9] H. Engan, "Excitation of elastic surface waves by spatial harmonics of interdigital transducers," *IEEE Trans. Electron Dev.*, vol ED-16, p. 1014–1017, 1969.
[10] T. I. Browning, and M. F. Lewis, "A novel technique for improving the temperature stability of SAW/SSBW devices," *Proc. 32nd Annu. Frequency Control Symp.*, p. 87, 1978.
[11] *IRE Standards on Electron Tubes: Definitions of Terms, 1957, Proc. IRE*, vol. 45, p. 1000, July 1957.
[12] *IRE Standards on Methods of Measuring Noise in Linear Two Ports, 1959, Proc. IRE.*, vol. 48, p. 60–68, Jan. 1960.
[13] Hewlett Packard Application Note 154, "S-parameter design," p. 26–27.
[14] J. H. Shoaf, D. Halford, and A. S. Risley, "Frequency stability specifications and measurements," NBS Tech., Note 632, Jan. 1973.
[15] A. L. Lance, W. D. Seal, F. G. Mendoza, and N. W. Hudson, "Automated phase noise measurements," *Microwave J.*, p. 87, June 1977.
[16] L. S. Cutler, and C. L. Searle, "Some aspects of the theory and measurement of frequency fluctuations in frequency standards," *Proc. IEEE*, vol. 54, p. 136–154, Feb. 1966.